

Yu-Lin Chen

List of Publications by Year in descending order

Source: <https://exaly.com/author-pdf/1897791/publications.pdf>

Version: 2024-02-01

85

papers

17,137

citations

76326

40

h-index

56724

83

g-index

90

all docs

90

docs citations

90

times ranked

15097

citing authors

#	ARTICLE	IF	CITATIONS
1	Experimental Realization of a Three-Dimensional Topological Insulator, Bi ₂ Te ₃ . Science, 2009, 325, 178-181.	12.6	3,095
2	Discovery of a Three-Dimensional Topological Dirac Semimetal, Na ₃ Bi. Science, 2014, 343, 864-867.	12.6	1,889
3	A stable three-dimensional topological Dirac semimetal Cd ₃ As ₂ . Nature Materials, 2014, 13, 677-681.	27.5	1,242
4	Direct observation of the transition from indirect to direct bandgap in atomically thin epitaxial MoSe ₂ . Nature Nanotechnology, 2014, 9, 111-115.	31.5	1,129
5	Massive Dirac Fermion on the Surface of a Magnetically Doped Topological Insulator. Science, 2010, 329, 659-662.	12.6	1,051
6	Giant anomalous Hall effect in a ferromagnetic kagome-lattice semimetal. Nature Physics, 2018, 14, 1125-1131.	16.7	876
7	Weyl semimetal phase in the non-centrosymmetric compound TaAs. Nature Physics, 2015, 11, 728-732.	16.7	796
8	Quantum spin Hall state in monolayer 1T'-WTe ₂ . Nature Physics, 2017, 13, 683-687.	16.7	596
9	Magnetic Weyl semimetal phase in a Kagomé crystal. Science, 2019, 365, 1282-1285.	12.6	518
10	High electron mobility and quantum oscillations in non-encapsulated ultrathin semiconducting Bi ₂ O ₂ Se. Nature Nanotechnology, 2017, 12, 530-534.	31.5	507
11	Bulk Fermi surface coexistence with Dirac surface state in $\text{Bi}_2\text{O}_2\text{Se}$. Nature Nanotechnology, 2017, 12, 530-534. A comparison of photoemission and Shubnikov-de Haas measurements. Physical Review B, 2010, 81, .	31.5	507
12	Signature of type-II Weyl semimetal phase in MoTe ₂ . Nature Communications, 2017, 8, 13973.	12.8	358
13	Linear Magnetoresistance Caused by Mobility Fluctuations in MoTe_2 . Physical Review Letters, 2015, 114, 117201.	7.8	306
14	Emergence of the nematic electronic state in FeSe. Physical Review B, 2015, 91, .	3.2	302
15	Giant, unconventional anomalous Hall effect in the metallic frustrated magnet candidate, KV ₃ Sb ₅ . Science Advances, 2020, 6, eabb6003.	10.3	295
16	Evolution of the Fermi surface of Weyl semimetals in the transition metal pnictide family. Nature Materials, 2016, 15, 27-31.	27.5	245
17	High-throughput calculations of magnetic topological materials. Nature, 2020, 586, 702-707.	27.8	241
18	Ultrafast and highly sensitive infrared photodetectors based on two-dimensional oxyselenide crystals. Nature Communications, 2018, 9, 3311.	12.8	213

#	ARTICLE	IF	CITATIONS
19	Single Dirac Cone Topological Surface State and Unusual Thermoelectric Property of Compounds from a New Topological Insulator Family. <i>Physical Review Letters</i> , 2010, 105, 266401.	7.8	195
20	Photonic topological insulator with broken time-reversal symmetry. <i>Proceedings of the National Academy of Sciences of the United States of America</i> , 2016, 113, 4924-4928.	7.1	193
21	Chiral topological semimetal with multifold band crossings and long Fermi arcs. <i>Nature Physics</i> , 2019, 15, 759-765.	16.7	184
22	Nontrivial Berry phase and type-II Dirac transport in the layered material $\text{xmlns:mml}=\text{"http://www.w3.org/1998/Math/MathML"} \langle \text{mml:mrow} \rangle \langle \text{mml:mi} \rangle \text{PdT} \langle / \text{mml:mi} \rangle \langle \text{mml:msub} \rangle \langle \text{mml:mi} \rangle \text{mathvariant}=\text{"normal"} \langle \text{e} \rangle \langle / \text{mml:mi} \rangle \langle \text{mml:mn} \rangle 2 \langle / \text{mml:mn} \rangle \langle / \text{mml:msub} \rangle \langle / \text{mml:mrow} \rangle \langle / \text{mml:math} \rangle .$ <i>Physical Review B</i> , 2017, 96, .	3.2	179
23	Patterning two-dimensional chalcogenide crystals of Bi ₂ Se ₃ and In ₂ Se ₃ and efficient photodetectors. <i>Nature Communications</i> , 2015, 6, 6972.	12.8	172
24	Electronic structures and unusually robust bandgap in an ultrahigh-mobility layered oxide semiconductor, Bi ₂ O ₂ Se. <i>Science Advances</i> , 2018, 4, eaat8355.	10.3	167
25	Electronic Structure, Surface Doping, and Optical Response in Epitaxial WSe ₂ Thin Films. <i>Nano Letters</i> , 2016, 16, 2485-2491.	9.1	147
26	Selectively enhanced photocurrent generation in twisted bilayer graphene with van Hove singularity. <i>Nature Communications</i> , 2016, 7, 10699.	12.8	136
27	<i>Review</i> Spin-orbit Coupling in the nonsymmorphic critical semimetals $\langle \text{mml:math} \rangle \text{xmlns:mml}=\text{"http://www.w3.org/1998/Math/MathML"} \langle \text{mml:mrow} \rangle \langle \text{mml:mi} \rangle \text{M} \langle / \text{mml:mi} \rangle \langle \text{mml:mi} \rangle \text{SiS} \langle / \text{mml:mi} \rangle \langle \text{mml:mspace} \text{width}=\text{"0.16em"} \rangle \langle \text{mml:mo} \rangle \langle \text{mml:mi} \rangle \text{M} \langle / \text{mml:mi} \rangle \langle \text{mml:mo} \rangle = \langle / \text{mml:mo} \rangle \langle \text{mml:mi} \rangle \text{Hf} \langle / \text{mml:mi} \rangle \langle \text{mml:mo} \rangle , \langle / \text{mml:mo} \rangle \langle \text{mml:mspace} \text{width}=\text{"0.16em"} \rangle \langle \text{mml:mo} \rangle \langle \text{mml:mi} \rangle \text{Hf} \langle / \text{mml:mi} \rangle \langle / \text{mml:mo} \rangle \langle / \text{mml:mspace} \text{width}=\text{"0.16em"} \rangle \langle / \text{mml:math} \rangle .$	3.2	131
28	<i>Review</i> Surface Monocrystallization of Copper Foil for Fast Growth of Large Singleâ€Crystal Graphene under Free Molecular Flow. <i>Advanced Materials</i> , 2016, 28, 8968-8974.	21.0	128
29	Hetero-site nucleation for growing twisted bilayer graphene with a wide range of twist angles. <i>Nature Communications</i> , 2021, 12, 2391.	12.8	92
30	Quantum oscillations of electrical resistivity in an insulator. <i>Science</i> , 2018, 362, 65-69.	12.6	79
31	Discovery of a single topological Dirac fermion in the strong inversion asymmetric compound BiTeCl. <i>Nature Physics</i> , 2013, 9, 704-708.	16.7	72
32	van Hove Singularity Enhanced Photochemical Reactivity of Twisted Bilayer Graphene. <i>Nano Letters</i> , 2015, 15, 5585-5589.	9.1	59
33	Molecular Beam Epitaxy and Electronic Structure of Atomically Thin Oxselenide Films. <i>Advanced Materials</i> , 2019, 31, e1901964.	21.0	59
34	Visualizing electronic structures of quantum materials by angle-resolved photoemission spectroscopy. <i>Nature Reviews Materials</i> , 2018, 3, 341-353.	48.7	58
35	Charge Density Wave Orders and Enhanced Superconductivity under Pressure in the Kagome Metal CsV ₃ Sb ₅ . <i>Advanced Materials</i> , 2021, 33, e2102813.	21.0	54
36	Building Large-Domain Twisted Bilayer Graphene with van Hove Singularity. <i>ACS Nano</i> , 2016, 10, 6725-6730.	14.6	53

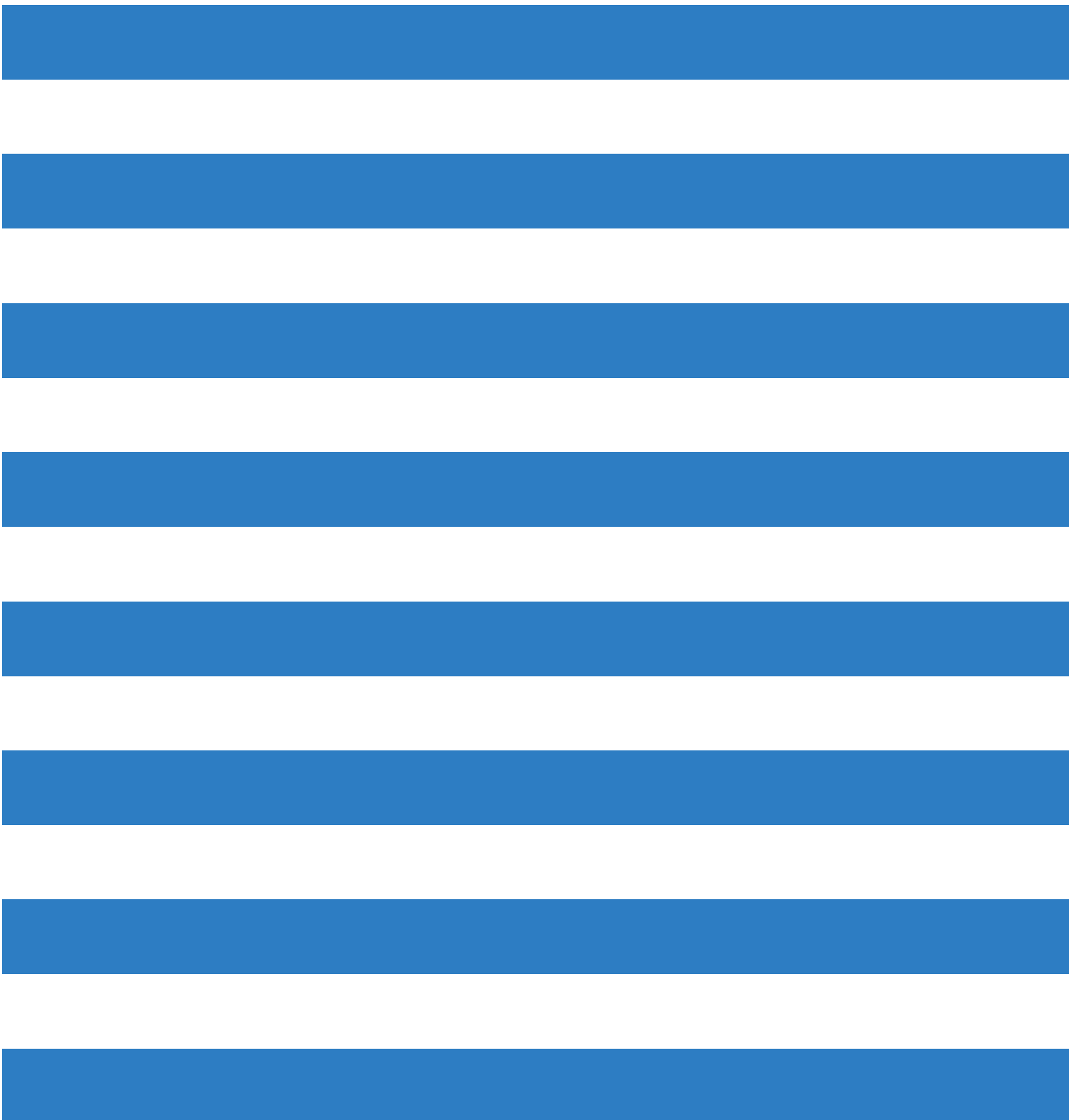
ARTICLE

Topological gapless Dirac cone and tunable topological states in C_{60}Fe_3

IF

CITATIONS

37



#	ARTICLE	IF	CITATIONS
55	A vacuum ultraviolet laser with a submicrometer spot for spatially resolved photoemission spectroscopy. <i>Light: Science and Applications</i> , 2021, 10, 22.	16.6	22
56	Strong spin-orbit coupling and Dirac nodal lines in the three-dimensional electronic structure of metallic rutile IrO_3 . <i>Physical Review B</i> , 2019, 99, .	3.2	18
57	Engineered heterostructures. <i>Nature Materials</i> , 2017, 16, 3-4.	27.5	16
58	Direct observation of the spin-orbit coupling effect in magnetic Weyl semimetal $\text{Co}_3\text{Sn}_2\text{S}_2$. <i>Npj Quantum Materials</i> , 2022, 7, .	5.2	16
59	Growth of BiSe and BiTe on amorphous fused silica by MBE. <i>Physica Status Solidi (B): Basic Research</i> , 2015, 252, 1334-1338.	1.5	15
60	Super resolution convolutional neural network for feature extraction in spectroscopic data. <i>Review of Scientific Instruments</i> , 2020, 91, 033905.	1.3	15
61	Lifshitz Transitions Induced by Temperature and Surface Doping in Type-II Weyl Semimetal Candidate $\text{T}_{1-x}\text{d}_x\text{WTe}_2$. <i>Physica Status Solidi - Rapid Research Letters</i> , 2017, 11, 1700209.	2.4	14
62	Band-selective Holstein polaron in Luttinger liquid material $\text{A}_0.3\text{MoO}_3$ ($\text{A}=\text{K}, \text{Rb}$). <i>Nature Communications</i> , 2021, 12, 6183.	12.8	13
63	Topological Lifshitz transition of the intersurface Fermi-arc loop in NbIrTe_4 . <i>Physical Review B</i> , 2020, 102, .	1.2	11
64	Angle-Resolved Photoemission Spectroscopy Study of Topological Quantum Materials. <i>Annual Review of Materials Research</i> , 2020, 50, 131-153.	9.3	12
65	Quantum Oscillations in Noncentrosymmetric Weyl Semimetal SmAlSi . <i>Chinese Physics Letters</i> , 2022, 39, 047501.	3.3	12
66	Observing electronic structures on <i>ex-situ</i> grown topological insulator thin films. <i>Physica Status Solidi - Rapid Research Letters</i> , 2013, 7, 130-132.	2.4	10
67	Pressure-induced superconductivity and structure phase transition in Pt_2HgSe_3 . <i>Npj Quantum Materials</i> , 2021, 6, .	5.2	10
68	Electronic structure of the Si-containing topological Dirac semimetal $\text{Ca}_x\text{S}_y\text{Se}_z$. <i>Physical Review B</i> , 2020, 102, .	3.2	9
69	Exploiting Two-Dimensional $\text{Bi}_2\text{O}_2\text{Se}$ for Trace Oxygen Detection. <i>Angewandte Chemie</i> , 2020, 132, 18094-18099.	2.0	7
70	Evolution of electronic structure and electron-phonon coupling in ultrathin tetragonal CoSe films. <i>Physical Review Materials</i> , 2018, 2, .	2.4	7
71	Topological phase transition in a magnetic Weyl semimetal. <i>Physical Review B</i> , 2021, 104, .	3.2	7
72	Observation of dimension-crossover of a tunable 1D Dirac fermion in topological semimetal NbSixTe_2 . <i>Npj Quantum Materials</i> , 2022, 7, .	5.2	7

#	ARTICLE	IF	CITATIONS
73	A new topological insulator built from quasi one-dimensional atomic ribbons. <i>Physica Status Solidi - Rapid Research Letters</i> , 2015, 9, 130-135.	2.4	6
74	How to probe the spin contribution to momentum relaxation in topological insulators. <i>Nature Communications</i> , 2018, 9, 56.	12.8	5
75	Visualization of the electronic phase separation in superconducting $K_xFe_{2-y}Se_2$. <i>Nano Research</i> , 2021, 14, 823-828.	10.4	4
76	Surface photovoltaic effect and electronic structure of I_2 -InSe. <i>Physical Review Materials</i> , 2020, 4, .	2.4	3
77	Single crystalline electronic structure and growth mechanism of aligned square graphene sheets. <i>APL Materials</i> , 2018, 6, .	5.1	2
78	Electronic structures of topological quantum materials studied by ARPES. <i>Semiconductors and Semimetals</i> , 2021, 108, 1-42.	0.7	2
79	Direct Visualization and Manipulation of Tunable Quantum Well State in Semiconducting Nb_2SiTe_4 . <i>ACS Nano</i> , 2021, 15, 15850-15857.	14.6	2
80	Electronic structure of correlated topological insulator candidate YbB_6 studied by photoemission and quantum oscillation. <i>Chinese Physics B</i> , 2020, 29, 017304.	1.4	1
81	Observation of the critical state to multiple-type Dirac semimetal phases in $KMgBi$. <i>Journal of Applied Physics</i> , 2021, 129, .	2.5	1
82	Electronic structure of a thermoelectric material: $BiCuSO$. <i>Physical Review B</i> , 2021, 103, .	3.2	1
83	Electronic structure and spin-orbit coupling in ternary transition metal chalcogenides Cu_2TiX_2 ($X = Se, Te$). <i>Chinese Physics B</i> , 2022, 31, 037101.	1.4	0
84	Measurement of the electronic structure of a type-II topological Dirac semimetal candidate VAl_3 using angle-resolved photoelectron spectroscopy. <i>Tungsten</i> , 0, , 1.	4.8	0
85	Observation of nontrivial topological electronic structure of orthorhombic $SnSe$. <i>Physical Review Materials</i> , 2022, 6, .	2.4	0